Indonesian Journal of Electrical Engineering and Computer Science
Vol. 27, No. 2, August 2022, pp. 722~727
ISSN: 2502-4752, DOI: 10.11591/ijeecs.v27.i2.pp722-727

Luminescence and transfer for power characteristics of $Sr_4La(PO_4)_3O:Ce^{3+}$, Tb^{3+}, Mn^{2+} phosphor for WLEDs

My Hanh Nguyen Thi[1], Phan Xuan Le[2]
[1]Faculty of Mechanical Engineering, Industrial University of Ho Chi Minh City, Ho Chi Minh City, Vietnam
[2]Faculty of Mechanical - Electrical and Computer Engineering, School of Engineering and Technology, Van Lang University, Ho Chi Minh City, Vietnam

Article Info

Article history:

Received Nov 28, 2021
Revised Jun 5, 2022
Accepted Jun 23, 2022

Keywords:

Color rendering index
Lumen efficacy
Mie-scattering theory
$Sr_4La(PO_4)_3O:Ce^{3+}$, Tb^{3+}, Mn^{2+}
WLEDs

ABSTRACT

We apply the high-heat solid-state technique to create a sequence of phosphors $Sr_4La(PO_4)_3O$: Ce^{3+}, Tb^{3+}, Mn^{2+}. In $Sr_4La(PO_4)_3O$ the luminescence characteristics, heat resistance, and transfer of energy between Ce^{3+} and Tb^{3+} as well as Mn^{2+} were thoroughly studied. The insertion of the sensitizer Ce^{3+} ions can significantly flatter the emission of the color green from Tb^{3+} and the emission of the color red from Mn^{2+} via energy transfer. By modifying the Ce^{3+}/Tb^{3+} and Ce^{3+}/Mn^{2+} ion ratios, it can change the emission color. White light, which has color coordinates of 0.3326, 0.3298, were produced by the $Sr_4La(PO_4)_3O$: $0.12Ce^{3+}$, $0.3Mn^{2+}$ $0.12Ce^{3+}$, $0.3Mn^{2+}$ specimen, showing $Sr_4La(PO_4)_3O:Ce^{3+}$, Tb^{3+}, Mn^{2+} might be profitable in white LEDs.

Corresponding Author:

Phan Xuan Le
Faculty of Mechanical - Electrical and Computer Engineering, School of Engineering and Technology, Van Lang University
Ho Chi Minh City, Vietnam
Email: le.px@vlu.edu.vn

1. INTRODUCTION

White-light-emitting diodes (WLEDs), which stand for diode emits white lighting, are broadly utilized and have garnered significant commercial popularity as solid-state lights as they offer extended lifespan, reduced energy usage, compact size, and ecological friendliness [1]-[3]. Creating a merger between a blue-colored InGaN chip and $Y_3Al_5O_{12}:Ce^{3+}$ or YAG:Ce that emits yellow light has recently become the greatest method for producing white emitting light [4]. Because lack of red-light components, this type of white light emission yields small CRI of roughly 70-80 as well as a better correlated color temperature (CCT) of roughly 7500 K [5]-[7]. Many researchers have focused in recent years on the study of blue light igniting phosphors to emit red lighting. $Na_5Ln(MoO_4)_4:Eu^{3+}$ (Ln = La, Gd, Y) [8], $CaS:Eu^{2+}$ [9], $CaAlSiN_3:Eu^{2+}$ [10] and $K_2SiF_6:Mn^{4+}$ [11]-[13] are illustrations of those phosphors. The WLEDs conversed phosphor can have poor CCT value and high color rendering index (CRI) value using these phosphors. Unfortunately, there are two key problems: high manufacturing costs and low blue-color radiation efficacy owing to considerable re-absorption between green-emitting and red-emitting phosphors. As a result, several investigations have concentrated on producing efficient, long-lasting, solitary white-light phosphors with red, green, and blue (RGB) elements using the energy transmission (ET) process from sensitizers to activators [14]-[16]. In various types of WLED phosphors, co-doping Ce^{3+}, Tb^{3+}, or Mn^{2+} ions is a popular technique for generating white luminescence via ET in solitary phosphors [17]-[19]. Ce^{3+} has a $4f^15d^0$ ground state and a $4f^05d^1$ excited state, allowing for standard symmetry allowed 5d-4f transitions of electricity. Because the host lattice strongly influences the distribution of Ce^{3+} energy levels, emission from the 5d-4f transition could occur over a large wavelength span. The ions Tb^{3+} and Mn^{2+} have both been employed as green and red radiation elements in the past. Nevertheless, owing to the prohibited 4f-4f transition of Tb^{3+} and $^4T_1$- $^6A_1$ transition of Mn^{2+}, the excitation bands of Tb^{3+} and Mn^{2+} ions from ultraviolet (UV) rays to the display area are fairly faint [20], [21]. Adding an effective sensitizer, including Ce^{3+}, and then transferring the significant stimulation energy of absorption from Ce^{3+} 5d's level to Tb^{3+}, $^5D_{3,4}$ levels or Mn^{2+} 4G's level is a popular technique to increase Tb^{3+} and Mn^{2+} absorption in the UV area [22]. This approach enables the manufacture of emission-tunable solitary phosphors, which have advantages namely lower production costs, better color reproducibility, and great luminescence efficacy [23].

Apatites have been proved to have a positive effect to host elements for phosphors in the past [24] as they possess excellent thermal and chemical consistency. The apatite complex $Sr_4La(PO_4)_3O$ (SLPO) contains two cationic zones: a nine-time coordination 4f location having C_3 point symmetry as well as a seven-time coordination 6h location having C_s point symmetry. The SLPO: $Eu^{3+}/Tb^{3+}/Ce^{3+}$ phosphors were investigated in prior research [25]. This study combined Tb^{3+} or Mn^{2+} with SLPO: Ce^{3+}. Using ET, a green color emission maximum of Tb^{3+} was obtained at 539 nm, as well as a red radiation range of Mn^{2+} has a peak at about 605 nm. From Ce^{3+} towards Tb^{3+} and Mn^{2+}, their photoluminescence characteristics and ET behaviors were extensively investigated. By varying the dopant Tb^{3+} concentration or Mn^{2+}, tunable emission hues spanning from blue-color to green-color and warmer white have been produced, hinting at a potential application in UV-pumped WLEDs.

2. COMPUTATIONAL SIMULATION

In this research, we use conventional high-temperature solid-state processes to produce $Sr_4La_{1-x-y}(PO_4)_3O$: xCe^{3+}, yTb^{3+} and $Sr_{4-z}La_{1-x(}PO_4)_3O$: xCe^{3+}, zMn^{2+} phosphors with various compositions. $SrCO_3$ (99.99%), $(NH_4)_2HPO_4$ (99.99%), La_2O_3 (99.99%), Tb_4O_7 (99.99%), $MnCO_3$ (99.99%), and CeO_2 (99.99%) were among the beginning components. And 2 wt% Li_2CO_3 (99%) worked as a flux. Then, completely combine and grind an agate mortar with the stoichiometric starting reagents. Pre-fired the mixture in the air for 3 hours at 600 °C, ground it again, and calcined it for 5 hours at 1200 °C in a decreasing atmosphere (N2 : H2 = 95 : 5). The optimal linear matching around the absorption peak may be attained when n = 2 in the plots of $[F(R)hv]^2$, $[F(R)h]$, $[F(R)h]^{2/3}$, $[F(R)h]^{1/2}$, and $[F(R)h]^{1/3}$ through the energy of photon *hv*. The plot of *[F(R)h]* versus *hv* can be seen via Figure 1. Generalizing the linear fit to *[F(R)h] = 0* yields the SLPO optic band gap energy (3.85eV).

Figure 1. Photograph of WLEDs

The absorption spectra of SLPO were attained from its reflecting band of colors in which the Kubelka-Munk (K-M) function was used to compute the optic bandgap value of the SLPO molecule analytically [26].

$$F(R) = \frac{(1-R)^2}{2R} = K/S \quad (1)$$

The reflection, absorption, as well as scattering coefficients, would be R, K, and S, respectively. The Taucrelation is a relationship between a material's bandgap Eg and linear absorption coefficient [26]:

$$\alpha hv \propto (hv - E_g)^{n/2} \quad (2)$$

where the photon energy is denoted by v, and n = 1, 2, 3, 4, and 6 denote direct transitions, non-metallic substances, directly banned transitions, indirectly allowed transitions, and indirectly forbidden transitions, respectively. The optic absorption K equals 2α when the substance disperses totally diffusely. Because the scattering coefficient S is proportional to the wavelength, (1) and (2) could be expressed as (3).

$$[F(R)hv]^2 \propto \left(hv - E_g\right)^n \quad (3)$$

Flat silicone layers replicate the phosphor layer of the genuine multi-chip white LED (MCW-LEDs) using the LightTools 9.0 application and the Monte Carlo approach. This simulation takes place through two different periods: i) it is important to establish and create MCW-LED lamp configuration models and optical characteristics; ii) the optical impacts of phosphor compounding are then properly controlled by the SLPO:Ce^{3+}, Tb^{3+} concentration variety. We must establish several contrasts to determine the YAG:Ce^{3+} effect and SLPO:Ce^{3+}, Tb^{3+} phosphor combining on the emission of MCW-LED lamps. Dual-layer distant phosphorus, described as two types of compounds with the average value of CCTs of 3000 K, 4000 K, and 5000 K, is to be elucidated. Figure 1 depicts MCW-LED lights using a protective-coating phosphor compound and a CCT value of 8500 K in detail. The simulation of MCW-LEDs without SLPO:Ce^{3+}, Tb^{3+} is also recommended. The reflector's length, pitch, and top exterior are 8 mm, 2.07 mm, and 9.85 mm, respectively. Nine chips with a width of 0.08 mm are treated with conformal phosphor compounds. All chips are connected to the reflector's gap via a square zone of 1.14 mm^2 and a 0.15 mm pitch. Each blue chip has a 1.16 W radiant flux with a 453 nm maximum wavelength.

3. RESULTS AND ANALYSIS

Figure 2 illustrates the reversal shift in the concentrations of green-emitting phosphor SLPO:Ce^{3+}, Tb^{3+}, and yellow emitting phosphor YAG:Ce^{3+}. This modification has two purposes: one is to keep the average value of CCTs, and one involves altering the absorbing activity as well as dispersion of the WLED device with two films of phosphor. This, in turn, has an impact on the WLED color standard and illuminating beam. WLEDs color quality is thus determined by the SLPO:Ce^{3+}, Tb^{3+} concentration chosen. When the SLPO:Ce^{3+}, Tb^{3+} ratio increased (2%-20% Wt.), the concentration of YAG:Ce^{3+} declined to keep the median value of CCTs. WLEDs with color heats ranging 5600-8500 K are no exception.

Figure 3 depicts the influence of the SLPO:Ce^{3+}, Tb^{3+} green-emitting phosphor concentration on WLEDs transmittance spectrum. It is feasible to decide after considering the producer's requirements. WLED devices with good hue fidelity may diminish luminous flux slightly. As shown in Figure 3, white light is the spectral region's synthesis. This diagram depicts a 5000 K spectrum. Obviously, the strength trend rises with concentration SLPO:Ce^{3+}, Tb^{3+} in two sections of the light spectrum: 420-480 nm along with 500-640 nm. Such a luminous flux rise may be seen in the two-band emission spectrum. Furthermore, blue-light dispersion increased in WLEDs, meaning that dispersion in the phosphorous film, and WLEDs will also rise, favoring color uniformity. When SLPO:Ce^{3+}, Tb^{3+} is presented, this is a significant outcome. The remote phosphor structure has the color uniformity of at high temperatures, in particular, is difficult to manage. This study found that SLPO:Ce^{3+}, Tb^{3+}, at both low and great color temperatures range of 5600 K and 8500 K, can enhance the WLEDs color standard. The efficiency of the emitted light flux of this dual-layer distant phosphor layer was further demonstrated in the paper. The results in Figure 4 demonstrate that the luminous flux emitted rose considerably as the concentration of SLPO:Ce^{3+}, Tb^{3+} grow from 2% wt to 20% wt. In all three average CCTs, the color divergence was enormously reduced with the phosphor SLPO:Ce^{3+}, Tb^{3+} concentration in Figure 5. The red-emitting phosphor layer's absorption is the explanation for this event. The LED chip's blue light is transformed to green light when the SLPO:Ce^{3+}, Tb^{3+} phosphor absorbs it. The SLPO:Ce^{3+}, Tb^{3+} particles still embodied the yellow light in addition to the LED chip's blue light. The blue illumination absorbed from the LED chip, though, is stronger than these two absorbs due to the material's absorption qualities. With the presence of SLPO:Ce^{3+}, Tb^{3+}, the green component in WLEDs rises, improving the color uniformity index. Color uniformity is among the most prominent factors among current WLED lamp parameters. The greater the color uniformity index is, the higher the cost of WLED. However, the low cost of SLPO:Ce^{3+}, Tb^{3+} is an advantage. SLPO:Ce^{3+}, Tb^{3+} can thus be used in a variety of applications.

Color uniformity is only one criterion to consider when assessing WLED color quality. Color quality is claimed to be badly affected by the color homogeneity index. As a result, recent studies have developed the CRI and the color quality scale (CQS). The actual color of an object is determined when light sheds on the CRI. The color discrepancy is caused by an excess of green illumination among three key hues green, blue, and yellow. This has an impact on the WLEDs color quality, resulting in a decrease in color fidelity. Figure 6 shows a modest fall in CRI when the distant phosphor SLPO:Ce^{3+}, Tb^{3+} layer is present.

Nonetheless, because CRI is simply a flaw in CQS, these are allowed. When comparing CQS and CRI, the CQS is far more necessary and harder to attain. CQS is a three-element index, with the first being the color rendering indicator, the second being beholder's choices, as well as the last being the hue coordinates. For these essentials elements, the CQS is nearly a genuine overall assessment of the color standard. As Figure 7 shows the increase of the CQS in the presence of the remote phosphor SLPO:Ce^{3+}, Tb^{3+} layer. When the SLPO:Ce^{3+}, Tb^{3+} concentration rise, CQS does not change considerably when the concentration of SLPO:Ce^{3+}, Tb^{3+} goes below 10% wt CRI, along with CQS, would be dramatically diminished when SLPO:Ce^{3+}, Tb^{3+} concentrations are larger than 10% wt, a result of severe waste of hue if the green color becomes dominant. Consequently, when utilizing green-color phosphor SLPO:Ce^{3+}, Tb^{3+}, proper concentration selection is critical.

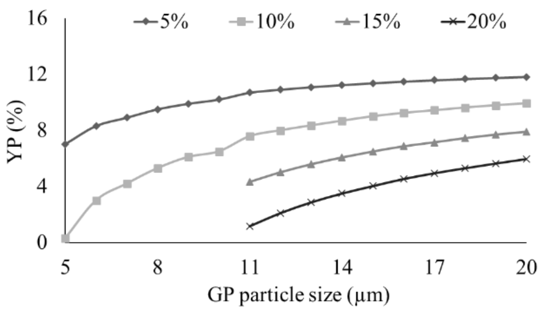

Figure 2. Altering particle size for the task of keeping median CCT

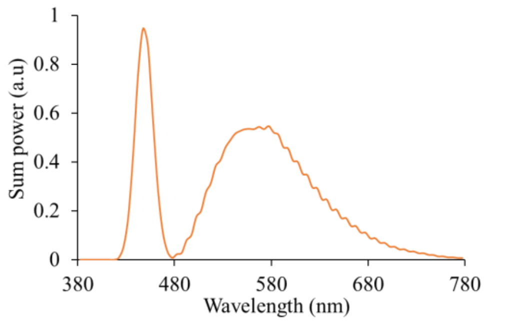

Figure 3. SLPO:Ce^{3+}, Tb^{3+} concentration functions as spectrum of LED package

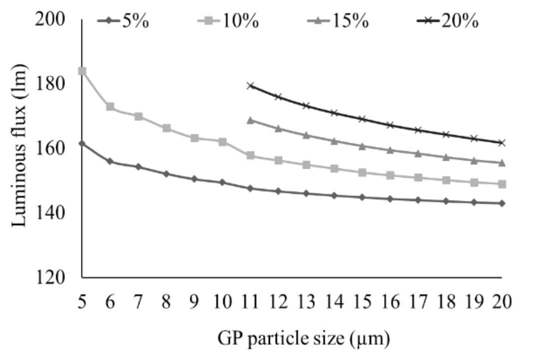

Figure 4. Concentration of SLPO:Ce^{3+}, Tb^{3+} in the form of lumen in the WLED device

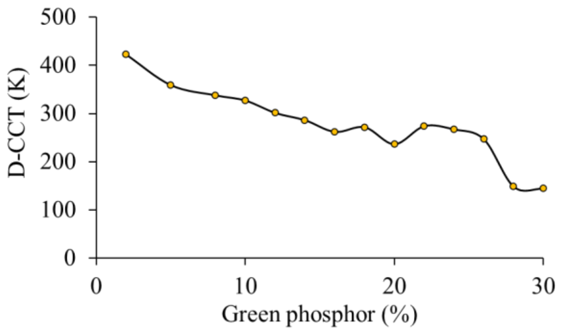

Figure 5. Concentration of SLPO:Ce^{3+}, Tb^{3+} in the form of hue aberration in the WLED device

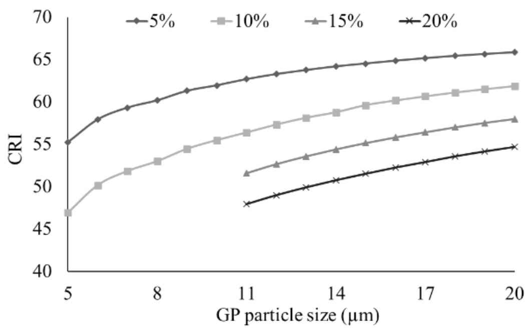

Figure 6. Concentration of SLPO:Ce^{3+}, Tb^{3+} in the form of color rendering indicator in the WLED device

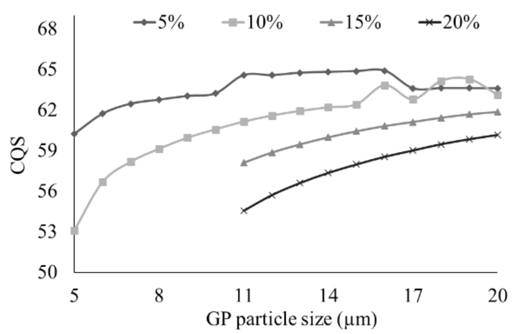

Figure 7. Concentration of SLPO:Ce^{3+}, Tb^{3+} in the form of hue standard scale in the WLED device

4. CONCLUSION

The effect of SLPO:Ce^{3+}, Tb^{3+} green phosphorus on the optical properties of a dual-layer phosphorus arrangement is the topic of this work. The study found that SLPO:Ce^{3+}, Tb^{3+} is a good selection for improving color homogeneity based on Monte Carlo computational simulations. It is true for WLEDs that have a color temperature of less than 5000 K and those of more than 8500 K. Because of the distant setup of phosphorus, the results of this article were able to augment the color output as well as lumen, seen as a difficult task. CRI and CQS, on the other hand, have a tiny drawback. The CRI and CQS fall dramatically when the SLPO:Ce^{3+}, Tb^{3+} concentration increase excessively. As a result, the right concentration must be chosen based on the manufacturer's aims. The article has provided an excellent deal of handy knowledge for generating higher color homogeneity and illuminating beam WLEDs.

ACKNOWLEDGEMENTS

This study was financially supported by Van Lang University, Vietnam.

REFERENCES

[1] Y. Liang *et al*., "Phosphor-in-glass (PIG) converter sintered by a fast Joule heating process for high-power laser-driven white lighting," *Optics Express*, vol. 29, no. 10, pp. 14218-14230, 2021, doi: 10.1364/OE.419633.

[2] B. Wang, D. S. Li, L. F. Shen, E. Y. B. Pun, and H. Lin, "Eu^{3+} doped high-brightness fluorophosphate laser-driven glass phosphors," *Optical Materials Express*, vol. 9, no. 4, pp. 1749-1762, 2019, doi: 10.1364/OME.9.001749.

[3] H. Liu, Y. Shi, and T. Wang, "Design of a six-gas NDIR gas sensor using an integrated optical gas chamber," *Optics Express*, vol. 28, no. 8, pp. 11451-11462, 2020, doi: 10.1364/OE.388713.

[4] T. Y. Orudzhev, S. G. Abdullaeva, and R. B. Dzhabbarov, "Increasing the extraction efficiency of a light-emitting diode using a pyramid-like phosphor layer," *Journal of Optical Technology*, vol. 86, no. 10, pp. 671-676, 2019, doi: 10.1364/JOT.86.000671.

[5] J. Li, Y. Tang, Z. Li, X. Ding, L. Rao, and B. Yu, "Investigation of stability and optical performance of quantum-dot-based LEDs with methyl-terminated-PDMS-based liquid-type packaging structure," *Optics Letters*, vol. 44, no. 1, pp. 90-93, 2019, doi: 10.1364/OL.44.000090.

[6] M. J. Egan, A. M. Colón, S. M. Angel, and S. K. Sharma, "Suppressing the multiplex disadvantage in photon-noise limited interferometry using cross-dispersed spatial heterodyne spectrometry," *Applied Spectroscopy*, vol. 75, no. 2, pp. 208-215, 2021, doi: 10.1177/0003702820946739.

[7] J. X. Yang, D. S. Li, G. Li, E. Y. B. Pun, and H. Lin, "Photon quantification in Ho3+/Yb3+ co-doped opto-thermal sensitive fluotellurite glass phosphor," *Applied Optics*, vol. 59, no. 19, pp. 5752-5763, 2020, doi: 10.1364/AO.396393.

[8] Y. P. Chang, *et al*., "An advanced laser headlight module employing highly reliable glass phosphor," *Optics Express*, vol. 27, no. 3, pp. 1808-1815, 2019, doi: 10.1364/OE.27.001808.

[9] H. Q. T. Bui, *et al*., "High-performance nanowire ultraviolet light-emitting diodes with potassium hydroxide and ammonium sulfide surface passivation," *Applied Optics*, vol. 59, no. 24, pp. 7352-7356, 2020, doi: 10.1364/AO.400877.

[10] T. W. Kang, *et al*., "Enhancement of the optical properties of $CsPbBr_3$ perovskite nanocrystals using three different solvents," *Optics Letters*, vol. 45, no. 18, pp. 4972-4975, 2020, doi: 10.1364/OL.401058.

[11] A. S. Baslamisli and T. Gevers, "Invariant descriptors for intrinsic reflectance optimization," *Journal of the Optical Society of America A*, vol. 38, no. 6, pp. 887-896, 2021, doi: 10.1364/JOSAA.414682.

[12] G. Granet and J. Bischoff, "Matched coordinates for the analysis of 1D gratings," *Journal of the Optical Society of America A*, vol. 38, no. 6, pp. 790-798, 2021, doi: 10.1364/JOSAA.422374.

[13] A. Alexeev, J. P. M. G. Linnartz, K. Arulandu, and X. Deng, "Characterization of dynamic distortion in LED light output for optical wireless communications," *Photonics Research*, vol. 9, no. 6, pp. 916-928, 2021, doi: 10.1364/PRJ.416269.

[14] I. Fujieda, Y. Tsutsumi, and S. Matsuda, "Spectral study on utilizing ambient light with luminescent materials for display applications," *Optics Express*, vol. 29, no. 5, pp. 6691-6702, 2021, doi: 10.1364/OE.418869.

[15] N. C. A. Rashid, *et al*., "Spectrophotometer with enhanced sensitivity for uric acid detection," *Chinese Optics Letters*, vol. 17, no. 8, p. 081701, 2019, doi: 10.3788/COL201917.081701.

[16] J. Zhou and K. Qian, "Low-voltage wide-field-of-view lidar scanning system based on a MEMS mirror," *Applied Optics*, vol. 58, no. 5, pp. A283-A290, 2019, doi: 10.1364/AO.58.00A283.

[17] Z. Li, J. Zheng, J. Li, W. Zhan, and Y. Tang, "Efficiency enhancement of quantum dot–phosphor hybrid white-light-emitting diodes using a centrifugation-based quasi-horizontal separation structure," *Optics Express*, vol. 28, no. 9, pp. 13279-13289, 2020, doi: 10.1364/OE.392900.

[18] Y. Chang *et al*., "New scheme of LiDAR-embedded smart laser headlight for autonomous vehicles," *Optics Express*, vol. 27, no. 20, pp. A1481-A1489, 2019, doi: 10.1364/OE.27.0A1481.

[19] J. Hao, H.-L. Ke, L. Jing, Q. Sun, and R.-T. Sun, "Prediction of lifetime by lumen degradation and color shift for LED lamps, in a non-accelerated reliability test over 20,000 h," *Applied Optics*, vol. 58, no. 7, pp. 1855-1861, 2019, doi: 10.1364/AO.58.001855.

[20] Z. Huang, Q. Liu, M. R. Pointer, W. Chen, Y. Liu, and Y. Wang, "Color quality evaluation of Chinese bronzeware in typical museum lighting," *Journal of the Optical Society of America A*, vol. 37, no. 4, pp. A170-A180, 2020, doi: 10.1364/JOSAA.381498.

[21] A. Ferrero, B. Bernad, J. Campos, N. Richard, C. Fernández-Maloigne, and M. Melgosa, "Goniochromatic assessment of gray scales for color change," *Journal of the Optical Society of America A*, vol. 37, no. 8, pp. 1266-1275, 2020, doi: 10.1364/JOSAA.394170.

[22] Z. Huang *et al*., "Towards an optimum colour preference metric for white light sources: a comprehensive investigation based on empirical data," *Optics Express*, vol. 29, no. 5, pp. 6302-6319, 2021, doi: 10.1364/OE.413389.

[23] R. Fan, S. Fang, C. Liang, Z. Liang, and H. Zhong, "Controllable one-step doping synthesis for the white-light emission of cesium copper iodide perovskites," *Photonics Research*, vol. 9, pp. 694-700, 2021, doi: 10.1364/PRJ.415015.

[24] X. Xi *et al*., "Chip-level Ce:GdYAG ceramic phosphors with excellent chromaticity parameters for high-brightness white LED device," *Optics Express*, vol. 29, no. 8, pp. 11938-11946, 2021, doi: 10.1364/OE.416486.
[25] J. R. Beattie and F. W. L. Esmonde-White, "Exploration of Principal Component Analysis: Deriving Principal Component Analysis Visually Using Spectra," *Applied Spectroscopy*, vol. 75, no. 4, pp. 361-375, 2021, doi: 10.1177/0003702820987847.
[26] Y. Wang *et al*., "Tunable white light emission of an anti-ultraviolet rare-earth polysiloxane phosphors based on near UV chips," *Optics Express*, vol. 29, no. 6, pp. 8997-9011, 2021, doi: 10.1364/OE.410154.

BIOGRAPHIES OF AUTHORS

My Hanh Nguyen Thi received a Bachelor of Physics from An Giang University, VietNam, Master of Theoretical Physics And Mathematical Physics, Hanoi National University of Education, VietNam. Currently, she is a lecturer at the Faculty of Mechanical Engineering, Industrial University of Ho Chi Minh City, Viet Nam. Her research interests are Theoretical Physics and Mathematical Physics. She can be contacted at email: nguyenthimyhanh@iuh.edu.vn.

Phan Xuan Le received a Ph.D. in Mechanical and Electrical Engineering from Kunming University of Science and Technology, Kunming city, Yunnan province, China. Currently, He is a lecturer at the Faculty of Engineering, Van Lang University, Ho Chi Minh City, Viet Nam. His research interests are Optoelectronics (LED), Power transmission and Automation equipment. He can be contacted at email: le.px@vlu.edu.vn.